Astron. Astrophys. 194, 125–134 (1988)

ASTRONOMY AND ASTROPHYSICS

# The IRAS two-colour diagram as a tool for studying late stages of stellar evolution

**W.E.C.J. van der Veen and H.J. Habing**

Sterrewacht Leiden, P.O. Box 9513, 2300 RA Leiden, The Netherlands

Received June 9, accepted September 4, 1987

**Summary.** IRAS two-colour diagrams are used to study dust/gas envelope stars (DGE-stars). DGE-stars are thought to be situated at the top of the Asymptotic Giant Branch (AGB) and can in general be divided into stars with oxygen-rich and stars with carbon-rich circumstellar shells.

Stars with oxygen-rich circumstellar shells form a sequence in the IRAS two-colour diagram (60 μm/25 μm versus 25 μm/12 μm) which is interpreted as an evolutionary track for oxygen-rich stars at the top of the AGB that steadily increase their mass loss rate. This track is the same as found earlier for stars known as Mira-variables and OH/IR stars. Along this track we find an increase in variability, in agreement with the idea that pulsations and mass loss occur simultaneously.

All DGE-stars together populate a much larger area in the two-colour diagram. Stars with carbon-rich circumstellar shells are located in another part of the IRAS two-colour diagram; they have different dust properties. And then there are a large number of stars with a strong excess at 60 μm probably caused by cold dust at a large distance from the star; the excess suggests that there are discontinuities in the mass loss history. A possible cause for such discontinuities are thermal pulses predicted for evolution at the AGB. As suggested by several authors carbon-rich material is dredged up during a thermal pulse and this can cause the transformation of an oxygen-rich circumstellar shell into a carbon-rich one.

**Key words:** infrared: photometry – stars: evolution – stars: mass loss

## 1. Introduction

In this paper we study stars at the Asymptotic Giant Branch (AGB) using Infrared Astronomical Satellite (IRAS) photometric data at 12, 25 and 60 μm together with low resolution spectra between 8 and 24 μm and an infrared-variability indication. Stars at the top of the AGB are cool variable stars with large luminosities and mass loss rates exceeding $10^{-7} M_{\odot}$/yr. It is thought that dynamical pulsations form shock waves in the stellar photosphere and supply the energy to lift up the gas to regions that are cool enough for dust formation. The dust, which is accelerated by radiation pressure and leaves the star, mainly radiates at wavelengths between 2 and 100 μm. This implies that many sources have been seen by IRAS. In this paper we explore the hypothesis that IRAS two-colour diagrams in combination with data from the LRS catalogue and with information of the infrared-variability enable us to distinguish stars with oxygen-rich circumstellar shells from carbon-rich ones and to order stars according to their mass loss rate.

*Send offprint requests to:* W.E.C.J. van der Veen

## 2. Observations

The observations used in this paper have been obtained with the IRAS satellite (Neugebauer et al., 1984). The most important part of its mission was to carry out an infrared survey of the whole sky in four broad wavelength bands centered at 12, 25, 60 and 100 μm. The angular resolution was limited: from 0.′8 × 4.′5 at 12 μm to 3.′0 × 5.′0 at 100 μm. In total 3 surveys were made; they are called HCON1, HCON2 and HCON3, where HCON stands for "hours confirmation": each scan was reobserved within 36 h to confirm the detection that was made the first time. Between HCON1 and HCON2 there were two weeks; between HCON2 and HCON3 there were 6 months. The sky coverage for HCON1, HCON2 and HCON3 is 95, 95 and 72% respectively.

The IRAS flux densities published in the Point Source Catalogue (IRAS, 1985; to be named PSC) are an average of up to three HCON measurements. In the PSC the measured inband fluxes (expressed in $Wm^{-2}$) are transformed into flux densities at 12, 25, 60 and 100 μm (expressed in Jy) by assuming a flat energy spectrum ($\nu F_{\nu} = 1$) for all sources. If the energy distribution is known, the PSC fluxes can be colour corrected using Table VI.C.6 of the IRAS Explanatory Supplement (1985).

Taking into account problems as confusion and cirrus, each flux in the PSC was assigned a "quality number", $Q$, ranging from 1 to 3; $Q = 1$ indicates that the flux is only an upper limit, $Q = 2$ indicates fluxes or moderate quality with some missing detections, $Q = 3$ indicates that the flux is of good quality with no confirmation problems.

After comparison of the three HCON's each source was given a "variability number", VAR, ranging from 0 to 99; the larger the number the larger the probability that the source is variable. Of course these numbers have only statistical meaning, because they depend on the period and phase of the variability at the time of the observations. In general a source is called variable if VAR > 80.

Low resolution spectra between 8 and 23 μm were obtained of bright, well isolated point sources by a separate spectrograph that operated simultaneously with the survey instrument. An "LRS classification number" is given to about 5,200 of these spectra as

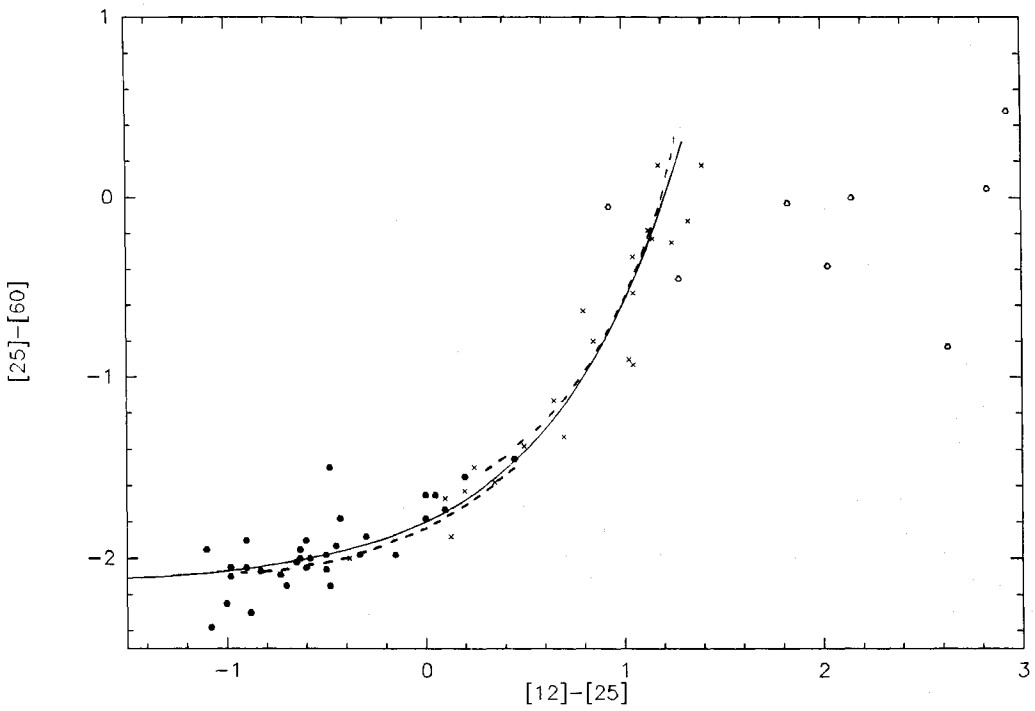


**Fig. 1.** IRAS two-colour diagram for a sample of Miras and OH/IR stars with good quality 12, 25, and 60 μm fluxes. The fit given by Eq. (2) is indicated by the full line

described in the IRAS LRS Catalogue (1986). The classification is based on the slope of the spectrum and the presence of certain lines between 8 and 13 μm.

Because the survey required only 60% of the available time, the remaining 40% was used for so called "additional observations". Here the survey instrument was used to do longer integrations on small parts of the sky to improve the signal-to-noise ratio. In this paper, however, we will only use the photometric data that are published in the PSC and in the LRS Catalogue.

To give an idea about the content of the PSC we have the following numbers (Chester, 1986). The PSC contains 282,000 point sources of which 158,000 (56%) are stars. Of these stars 18,000 objects have colours indicating the Rayleigh-Jeans tail of a Planck curve; 81,000 have colours that indicate the presence of circumstellar emission and 59,000 stars are too faint to characterize. Our interest mainly goes to those 81,000 stars with circumstellar emission from which we want to select stars with dust/gas envelopes that are on the AGB. In the rest of this paper these stars will be called dust/gas envelope stars (DGE-stars). OH/IR stars are the subsample of the DGE stars with detected 1612 MHz maser emission.

## 3. A representation of the IRAS data: the two-colour diagram

In this paper we present the IRAS photometric data at 12, 25, and 60 μm in the form of two-colour diagrams. Such diagrams have already been published by several authors (e.g. Olnon et al., 1984; Zuckerman and Dyck, 1986) and they appear to be well suited to study stars with circumstellar envelopes. We define two infrared colours, [12]–[25] and [25]–[60] respectively, as

$$[12]-[25] = 2.5\log\left(\frac{F_{25\,\mu m}}{F_{12\,\mu m}}\right); \quad [25]-[60] = 2.5\log\left(\frac{F_{60\,\mu m}}{F_{25\,\mu m}}\right) \qquad (1)$$

In the rest of this paper we will discuss the two-colour diagram defined by the colours given by Eq. (1). We will not apply a colour correction to these fluxes. In the first place the colour corrections are small and in many cases uncertain: at 12, 25, and 60 μm the correction is in the order of 10, 30, and 30% for Miras and 5, 10, 15% for OH/IR stars (Herman et al., 1986). The second reason is that the colour correction is only a one-to-one transformation of the axis in the two-colour diagram and will not change the global picture. For about the same reason no extinction correction will be applied. These corrections are small at wavelengths longer than 10 μm and uncertain because for most sources the distance is unknown.

### *3.1. The IRAS two-colour diagram for known Mira variables and OH/IR stars*

In this section we consider a subsample of DGE-stars that have oxygenrich circumstellar shells and that show OH emission at 1612 MHz. This group of stars forms a sequence of objects with gradually varying properties; extreme cases are optically visible, oxygen-rich, Mira variables and OH/IR stars of which the central star is totally obscured. Figure 1 shows the position in the two-colour diagram of a sample of well known Miras and OH/IR stars that have accurate fluxes at 12, 25, and 60 μm (all have $Q = 3$ for the three wavelength bands).

The Mira variables are indicated by black dots; the OH/IR stars can be divided into two classes: OH/IR stars with large amplitude variations in the OH 1612 MHz line are indicated by crosses; OH/IR stars with small or no amplitude variations in the OH 1612 MHz line, the so called "non-variable" OH/IR stars (Habing et al., 1987), are indicated by the open circles. The Miras and OH/IR stars clearly form a sequence from the lower left to the upper right. The sequence is well defined taking into account the inaccuracies in the infrared colours that are in the order of 0.15.

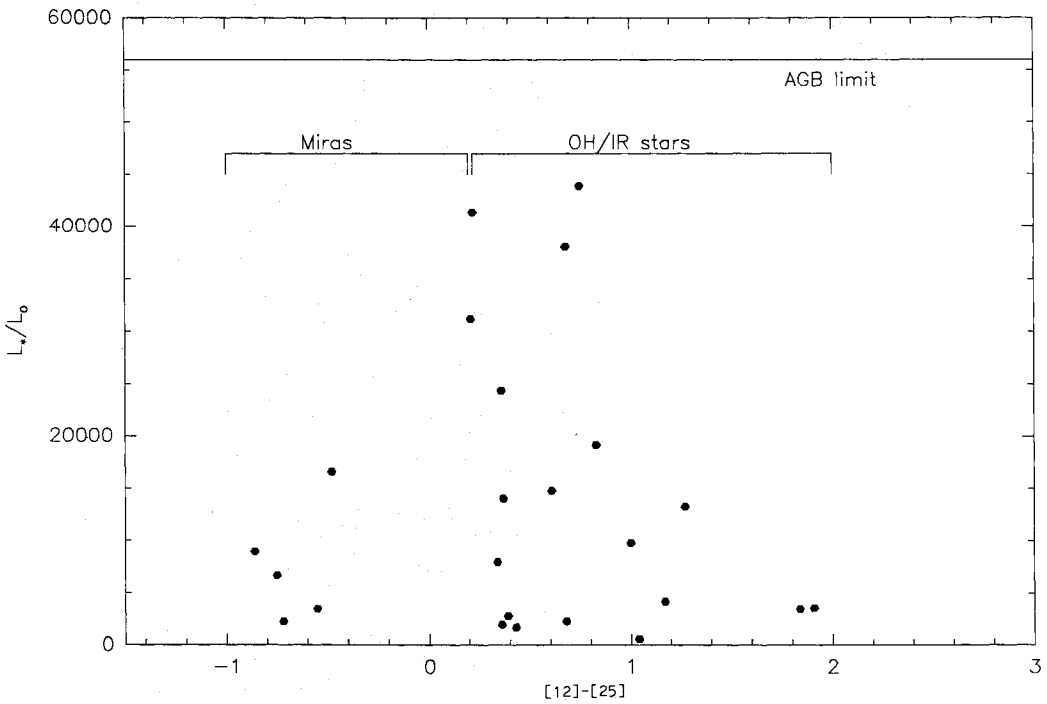


**Fig. 2.** Diagram of luminosity versus [12]–[25] colour for a sample of 25 Miras and OH/IR stars of which accurate distances are known

There is also a clear separation between the Miras and the OH/IR stars: the Miras are concentrated on the lower left side of the diagram; the OH/IR stars on the upper right side. The transition between Miras and OH/IR stars take place around [12]–[25] = 0.2; the transitions between "variable" OH/IR stars and "non-variable" OH/IR stars around [12]–[25] = 1.5.

Bedijn (1987) and Rowan-Robinson et al. (1986) have shown that the sequence from the Mira variables to the variable OH/IR stars represents a continuous sequence in mass loss rates ranging from $10^{-7}\,M_\odot$/yr at the lower left to more than $10^{-4}\,M_\odot$/yr at the upper right. Bedijn's result was obtained by assuming a central star with a temperature of 2500 K and a luminosity of 10,000 $L_\odot$ that is surrounded by an expanding circumstellar shell which is continuously fed at its inner radius by the mass losing central star. After solving the radiative transfer equation Bedijn reproduces the observed sequence in Fig. 1 by models with increasing mass loss rates (dashed line in Fig. 1). The "non-variable" OH/IR stars deviate from this sequence and their IRAS colours can not be reproduced by an increasing mass loss rate. Only the assumption that the central star has stopped to lose mass so that no new material is added at the inner shell radius yield colours that are in agreement with the observations.

The narrow sequence in Fig. 1 suggests that oxygen-rich Mira variables and variable OH/IR stars form a "one parameter family" in the two-colour diagram: only one of the IRAS colours is needed to find an estimate for their mass loss rate.

The curve in Fig. 1 (full line) which is given by

$$[25]\text{–}[60] = -2.15 + 0.35\exp(1.5([12]\text{–}[25])) \qquad (2)$$

represents the observed colours very well for [12]–[25] between −1.1 and 1.3.

There are two possible explanations for this observed sequence in mass loss rates.

*i*) The difference in mass loss rate reflects a difference in initial mass. Stars with small main sequence masses develop small mass loss rates on the AGB and show up as Miras. The more massive stars develop larger mass loss rates on the AGB and show up as OH/IR stars. When the enhanced mass loss ($\dot{M} > 10^{-8}\,M_\odot$/yr) starts they move to a certain point in the two-colour diagram in about one dynamical timescale (~200–1000 yr). They will stay at that point in the two colour diagram until their total envelope is lost. Because the more massive stars are expected to have larger luminosities on the AGB a correlation between infrared colour and luminosity (= mass) is also expected in this case. In Fig. 2 we have plotted 25 stars for which luminosities are determined by Herman et al. (1986). The distances that were used are "phase lag" – or "far kinematic" distances with an accuracy of 20–30%. Although this sample is certainly not complete it is clear from Fig. 2 that no correlation between the [12]–[25] colour and luminosity exists. There are no luminous Miras present in the sample, but there are a large number of low luminosity OH/IR stars with about the same luminosities as the Miras.

*ii*) The difference in mass loss rate reflects an evolution in mass loss. A star of given mass starts on the lower left side of the diagram as a Mira and evolves to the upper right to become an OH/IR star. This means that the mass loss rate is not stationary but evolving. Indications for non-stationary mass loss were already found by Baud and Habing (1983) from OH observations and by Bedijn (1987) who obtained better fits to the spectra at the long infrared wavelengths ($\lambda > 25\,\mu$m) assuming a density gradient steeper than the one for stationary outflow ($\varrho \sim r^{-2}$). The differences are small but systematic.

In the rest of this paper we will follow the second interpretation. The line represented by Eq. (2) will be reffered to as the "evolutionary track" from oxygen-rich Miras to OH/IR stars.

### *3.2. The IRAS two-colour diagram for DGE-stars with LRS spectra*

In this section we discuss all infrared sources in the PSC with good quality fluxes ($Q = 3$) that have an LRS spectrum which is typical

for a stellar object; a total of 3800 IRAS sources are plotted. As can be seen from comparison of the Figs. 1 and 3a, these objects populate a much larger area in the two-colour diagram than the Mira variables and OH/IR stars that are discussed in the preceeding section.

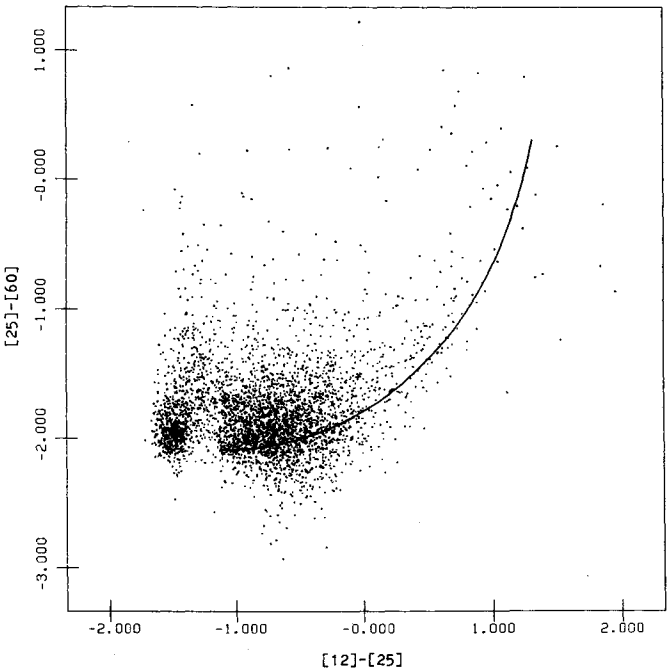


**Fig. 3a.** IRAS two-colour diagram for a sample of DGE-stars with LRS spectra that are typical for stellar objects with or without circumstellar emission; total number of objects is 3800. The "evolutionary track" of Fig. 1 is indicated by the full line

The "evolutionary track" as given by Eq. (2) is indicated by the full line. According to the LRS catalogue (1986) the following groups of stellar objects can be distinguished:

*(1)* Stellar photospheres with temperatures above 2000 K. They have LRS classification numbers 17–19 indicating that $S_\lambda \sim \lambda^{-3.5}$ (class 17) to $S_\lambda \sim \lambda^{-4.5}$ (class 19) between 8 and 13 μm.

*(2)* Stars with small amounts of circumstellar material. They have LRS classification numbers 14–16 indicating that $S_\lambda \sim \lambda^{-2}$ (class 14) to $S_\lambda \sim \lambda^{-3}$ (class 16) between 8 and 13 μm.

*(3)* Stars with oxygen-rich circumstellar shells that are still optical thin. They all show a 10 μm emission due to SiO condensed onto dust grains. The LRS classification numbers range from 21 to 29; from weak emission to very strong emission at 10 μm.

*(4)* Stars with oxygen-rich circumstellar shells that are optical thick. They all show a 10 μm absorption due to SiO condensed onto dust grains. The LRS classification numbers range from 31 to 39; from weak absorption to very strong absorption at 10 μm.

*(5)* Stars with carbon-rich circumstellar shells that are still optical thin. They all show a 11.3 μm emission feature. The LRS classification numbers range from 41 to 49; from weak emission to very strong emission.

We did not mention the LRS main classes 6 and 7 that contain only a small number of stars. They are the same as the main classes 2 and 3, but with a redder spectrum between 14 and 22 μm. Most objects in class 7 are compact H II-regions (LRS catalogue, 1986). Only a few of them are associated with a very red OH/IR star. The objects in LRS class 6 are sometimes associated with Mira-type objects or planetary nebulae, but in most of the cases the type of the associated object is not clear.

For all objects with a given LRS-classification we have calculated the average of the [12]–[25] and the [25]–[60] colour, the average position in the two-colour diagram and the average of the variability number (Fig. 3b).

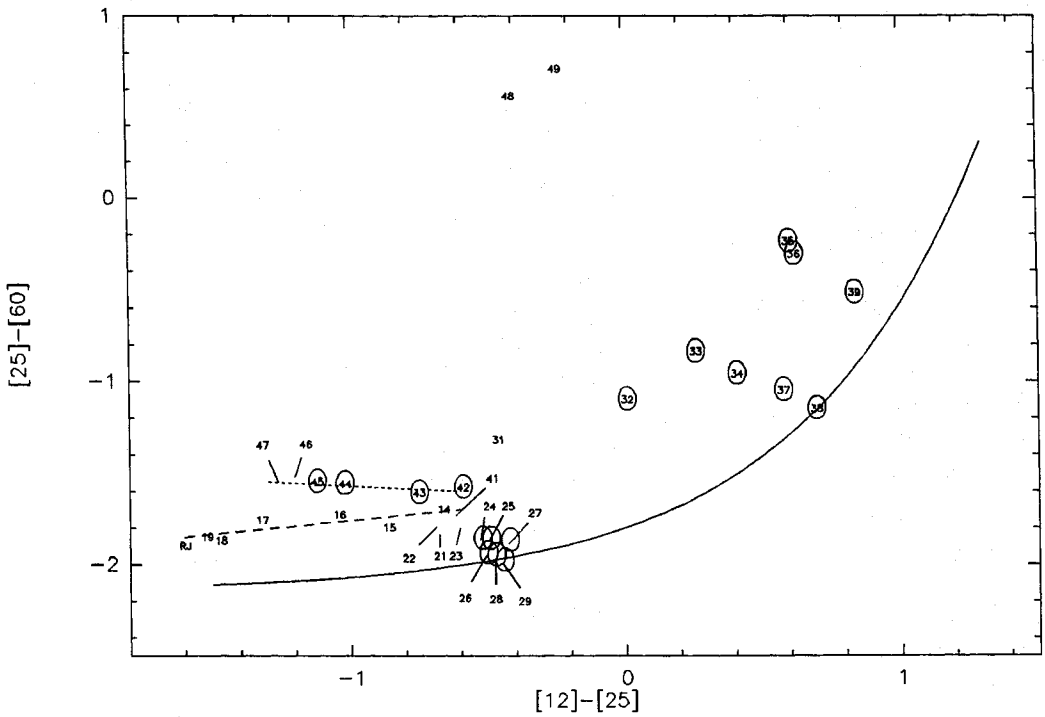


**Fig. 3b.** Averaged position of LRS-classes in the IRAS two-colour diagram. The "evolutionary track" of Fig. 1 is indicated by the full line. Evolutionary tracks for stars with featureless spectra (long-dashed line) and stars with 11.3 μm emission (short-dashed line) are also indicated

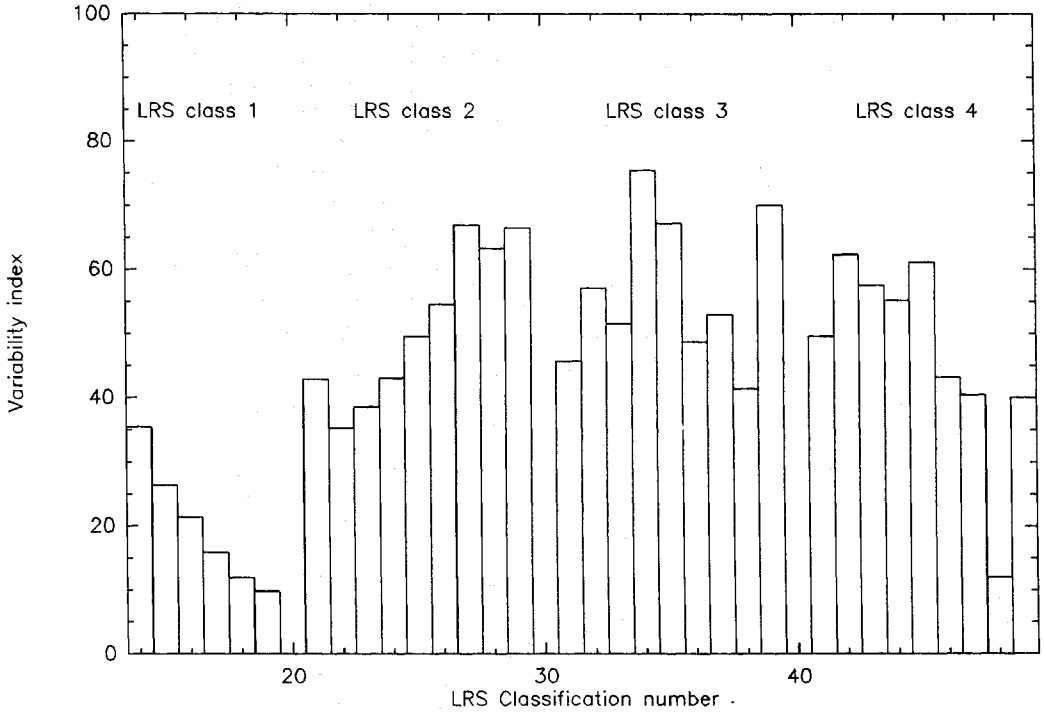


**Fig. 4.** Variability index for LRS-classes 1 to 4. Main class 1: stars with no feature; subclass 1–9: decreasing IR excess. Main class 2: stars with 10 μm emission; subclass 1–9: increasing strength. Main class 3: stars with 10 μm absorption; subclass 1–9: increasing strength. Main class 4: stars with 11.3 μm emission; subclass 1–9: increasing strength

The numbers within circles indicate LRS-classes with a variability average, ⟨VAR⟩, larger than 50. About 70% of the objects in a given LRS-class can be found within a radius of 0.2–0.4 magnitudes from the given position in the two-colour diagram. The exceptions are the objects in the classes 31, 48 and 49. The objects in class 31 are spread over a large part of the diagram, which is mainly caused by wrong classification as will be discussed further on. The classes 48 and 49 contain only 2 and 4 objects respectively of which only one has colours that are normal for a star with a circumstellar dust/gas shell.

On the lower left side of the diagram the Raleigh-Jeans point for stars is indicated by "RJ". From this point there is a track going to the right side of the diagram corresponding with an evolution of the LRS spectra from class 19 to 14: from $S_\lambda \sim \lambda^{-4.5}$ to $S_\lambda \sim \lambda^{-2}$. There is a good correlation between the average position of the subclasses 14 to 19 and the [12]–[25] colour. Along this track the [25]–[60] colour is almost constant which means that the infrared radiation is mainly from relatively hot dust close to the star. The track in the two-colour diagram (indicated by the long-dashed line) is given by

$$[25]\text{–}[60] = -1.61 + 0.15\,([12]\text{–}[25]);\ (-1.6 \leq [12]\text{–}[25] \leq -0.6). \quad (3)$$

The variability average of the classes 19 to 14 increases from ⟨VAR⟩ = 9.8 for LRS class 19 to ⟨VAR⟩ = 35.5 for LRS-class 14 as is shown in Fig. 4.

Such a correlation between variability and infrared colour is expected for stars with mass loss driven by stellar pulsations.

Starting from [12]–[25] = −1.3 we see a second track going to the right. It is situated at a larger [25]–[60] colour and corresponds with a decrease in strength of the 11.3 μm emission as follows from the decrease in LRS number from 47 to 42. This track (the short-dashed line in Fig. 3b) is given by

$$[25]\text{–}[60] = -1.64 - 0.07\,([12]\text{–}[25]);\ (-1.3 \leq [12]\text{–}[25] \leq -0.6). \quad (4)$$

On the average the [25]–[60] colour of these stars with carbon-rich shells is about 0.2 mag larger than for stars with oxygen-rich shells. This is caused by the different wavelength dependence of carbon- and oxygen-rich dust grains at wavelengths between 40 and 80 μm (e.g. Zuckermann and Dyck, 1986). The variability average increases from ⟨VAR⟩ = 40.5 for LRS class 47 to ⟨VAR⟩ = 62.3 for LRS class 42 as is shown in Fig. 4. The variability average of this group of objects is significantly larger than for the objects that are on the lower curve.

At the end of both tracks we find stars with LRS classifications 21–23, 31 and 41. These are all objects with very weak features which makes an accurate classification difficult (LRS catalogue, 1986). The variability average of these objects range between 40 and 50.

If we continue to slightly larger [12]–[25] colours we find a group of objects with 10 μm emission features which are clustered around [12]–[25] = −0.5 and [25]–[60] = −1.9; there is no correlation between the averaged position of the LRS classes and the infrared colours! The presence of the 10 μm emission indicates that these stars have oxygen-rich circumstellar shells. The larger [12]–[25] colour indicates that these stars have larger mass loss rates than the objects with LRS classes 19 to 14.

The variability average increases with increasing strength of the 10 μm feature from ⟨VAR⟩ = 38.6 for class 23 to ⟨VAR⟩ = 66.5 for class 29 as is shown in Fig. 4.

If we follow the "evolutionary track" from Mira variables to OH/IR stars (full line in Fig. 3b) to the upper right side of the two-

colour diagram we find objects with 10 μm absorption, indicating that they have very thick oxygen-rich circumstellar shells. The strength of the absorption tend to increase with increasing [12]–[25] colour. There is also an increase of the [25]–[60] colour as a function of the [12]–[25] colour which follows the "evolutionary track" from the oxygen-rich Mira variables to the OH/IR stars. Note that the strength of the 10 μm absorption tends to decrease if one moves away from this track to larger [25]–[60] colours.

Finally, Fig. 4 shows that there is no correlation between the variability average and the strength of the 10 μm absorption.

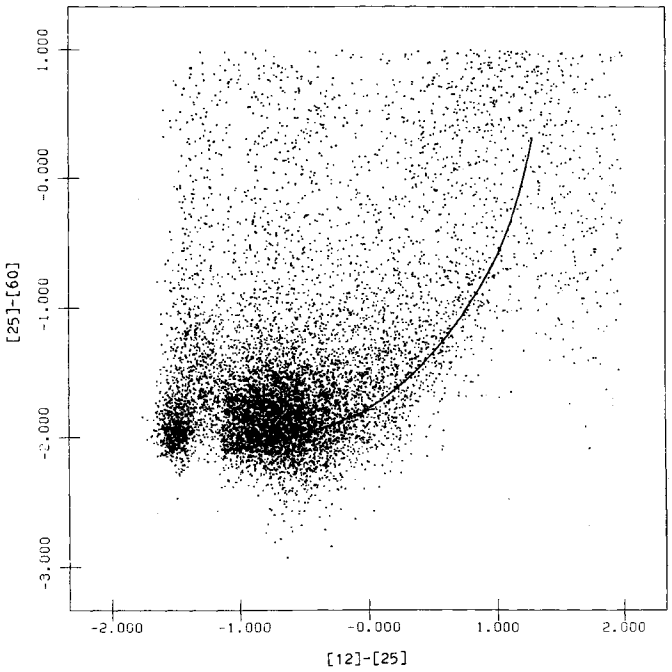


**Fig. 5a.** IRAS two-colour diagram for all IRAS point sources with good quality 12, 25 and 60 μm fluxes that have a [12]–[25] colour between −2.0 and 2.0 and a [25]–[60] colour between −3.0 and 1.0. Total number of objects is 8864

### 3.3. *The IRAS two-colour diagram for DGE-stars*

To see if the results of the preceeding section are characteristic for all IR-sources in the same part of the two-colour diagram, we have selected all sources from the PSC with good quality fluxes ($Q = 3$) and with a [12]–[25] colour between −2.0 and 2.0 and a [25]–[60] colour between −3.0 and 1.0. The two-colour diagram so obtained (Fig. 5a) contains 8864 objects with a variability average equal to 40.5; 43% of these objects have a LRS spectrum with a variability average equal to 40.2.

Figures 3a and 5a look the same except from the upper part of the diagram where the region for which [25]–[60] > −1 is now filled up with sources: the number of sources with [25]–[60] is increased by a factor of 9, whereas the number of sources with [25]–[60] > −1 is increased by only a factor of 2.

As a first step in the analysis we divided the diagram in squares of 0.2 × 0.2 magnitudes. For each square we calculated the total number of objects and the variability average. As a second step we divided the two-colour diagram into 10 regions as shown in Fig. 5b based on the infrared characteristics – number densities, the variability average and the LRS classification.

Characteristic properties of each of these regions are summarized in Table 1. For each region we checked the "associations" of the infrared sources as given in the PSC (see IRAS Explanatory Supplement, p. V. 65); the results are summarized in Table 2. We now discuss the regions one by one.

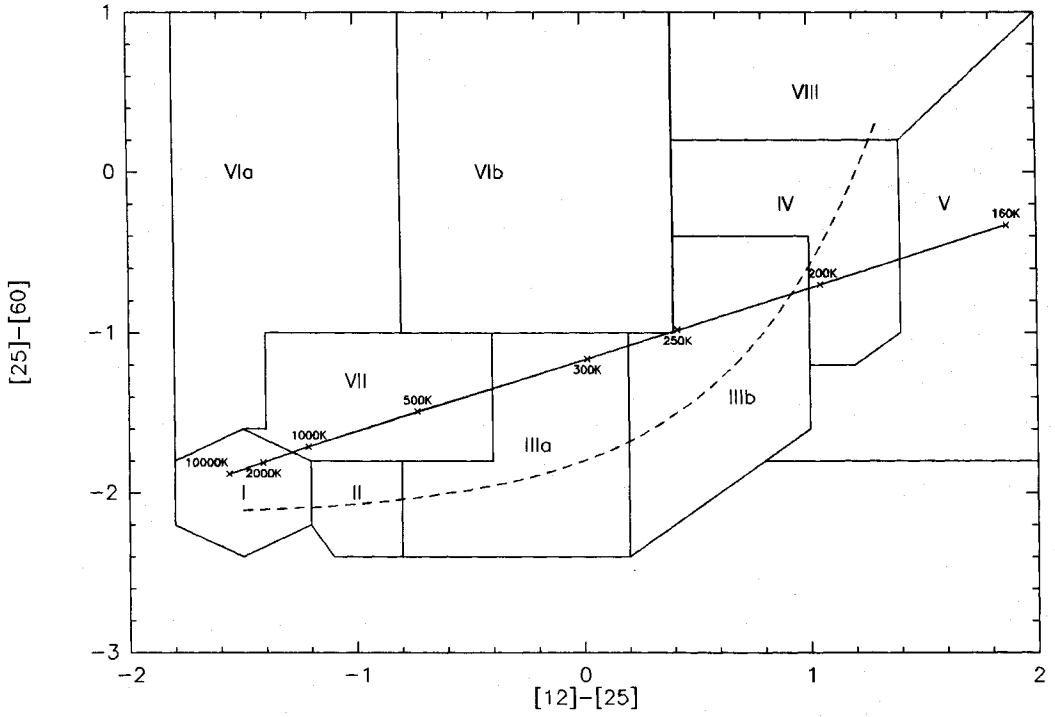


**Fig. 5b.** Regions in the IRAS two-colour diagram that separate different sort of DGE-stars (see text). The "evolutionary track" of Fig. 1 is indicated by the dashed line. The black body curve is indicated by the full line

**Table 1.** Star counts and averaged variability for different regions in the IRAS two-colour diagram as indicated in Fig. 5b

| Region | No. | ⟨VAR⟩ | No. (LRS) | LRS class | Characteristic type of object |
|---|---|---|---|---|---|
| I | 791 | 12.7 | 76% | 17–19 (89%) | Oxygen-rich non-variable stars without circumstellar shells |
| II | 869 | 35.0 | 65% | 14–16 (64%)<br>21–29 (23%) | Variable stars with "young" O-rich circumstellar shells |
| IIIa | 2657 | 55.1 | 55% | 21–29 (76%)<br>14–16 (14%) | Variable stars with more evolved O-rich circumstellar shells |
| IIIb | 617 | 64.7 | 20% | 31–39 (66%)<br>21–24 (11%)<br>41–43 ( 9%) | Variable stars with thick O-rich circumstellar shells |
| IV | 204 | 29.6 | 8% | 39 (50%)<br>71–79 (31%) | Variable stars with very thick O-rich circumstellar shells |
| V | 176 | 16.4 | 15% | 91–96 (69%)<br>71–79 (27%) | Planetary nebulae and non-variable stars with very cool circumstellar shells |
| VIa | 501 | 19.9 | 20% | 16–18 (64%)<br>42–45 (17%)<br>31–32 ( 8%) | Non-variable stars with relatively cold dust at large distances; a significant part of the stars is carbon-rich |
| VIb | 605 | 35.9 | 5% | 22–29 (47%)<br>14–15 (37%) | Variable stars with relatively hot dust close to the star and relatively cold dust at large distances; some of the objects have proven to be oxygen-rich |
| VII | 2048 | 40.6 | 44% | 41–47 (30%)<br>21–29 (22%)<br>14–16 (35%)<br>17–18 (11%) | Variable stars with more evolved C-rich circumstellar shells |
| VIII | 315 | 27.1 | 10% | 71–79 (43%)<br>91–95 (30%)<br>33–36 (13%) | Different sort of objects (see text) |

*Region I:* These objects are concentrated around the Rayleigh-Jeans point and we conclude that they represent stellar photospheres with temperatures above 2000 K. This agrees with LRS spectra: about 90% have Rayleigh Jeans type spectra without an IR-excess. The variability average is low (⟨VAR⟩ = 13). From Table 2 we see that 11% of the infrared sources are associated with a variable star and 26% with a suspected variable. Only 3% of the infrared sources are associated with a cool carbon star or an S-star.

We conclude that the objects in this region are mainly non-variable oxygen-rich stars without circumstellar shells.

*Region II:* These objects hve [12]–[25] colours that are 0.5 magnitudes larger than in region I. The [25]–[60] colours are about the same. This suggests the presence of reatively hot circumstellar dust. The same is found from the LRS spectra: 90% show weak circumstellar dust emission. For 30% of the sources the 10 μm emission band is present showing that the dust is oxygen-rich; for the other 70% no distinction between oxygen- and carbon-rich dust can be made. From Table 2 however, we find that only 2% is associated with a cool carbon star or S-star.

The variability average equals 36, which is about 3 times larger than for the non-variable stars in region I. This agrees very well with the larger fraction of infrared sources that is associated with a variable star (57%); most variables are Miras.

We conclude that the objects in this region are mainly variable stars with relative "young" oxygen-rich circumstellar shells.

*Region IIIa:* These objects show a small increase of the [25]–[60] colour as a function of the [12]–[25] colour. Such a behaviour is expected for objects which increasingly larger mass loss rates (dashed curve in Fig. 5b). About 90% of all LRS spectra indicate small or moderate dust emission. In 85% of these spectra we find features that are characteristic of oxygen-rich dust; for the remaining 15% we cannot distinguish between oxygen- and carbon-rich dust. From Table 2, however, we see that none of the infrared sources is associated with a carbon star or an S-star.

The variability average equals 55, which is larger than in the regions I and II. The fraction of infrared sources associated with a variable or suspected variable, however, is smaller than in region II (Table 2). This is probably caused by the fact that the stars in this region are more obscured by circumstellar dust than the stars

**Table 2.** Associations of infrared sources for the different regions in the IRAS two-colour diagram as indicated in Fig. 5b. (The values are %)

| Sort of objects | I | II | IIIa | IIIb | IV | V | VIa | VIb | VII | VIII |
|---|---|---|---|---|---|---|---|---|---|---|
| Variable stars | 11 | 57 | 18 | 3 | 7 | 2 | 15 | 8 | 25 | 9 |
| Suspected variable star | 26 | 7 | 6 | 1 | 2 | 2 | 9 | 3 | 7 | 5 |
| Faint red stars | 29 | 16 | 6 | – | 1 | 1 | 19 | 1 | 11 | – |
| Cool carbon stars | 2 | 1 | – | 1 | – | – | 19 | 1 | 11 | – |
| S-stars | 1 | 1 | – | – | – | – | 2 | – | 2 | – |
| Dark nebulae | – | – | 1 | 3 | 7 | 6 | 2 | 4 | 2 | 13 |
| Early type stars with emission lines | 1 | – | 1 | 2 | 4 | 8 | 1 | 6 | 2 | 4 |
| Planetary nebulae | – | – | – | 2 | 7 | 35 | – | 2 | – | 3 |
| Galaxies | – | – | – | – | – | – | – | – | – | 15 |
| Total of associations | 70 | 82 | 32 | 12 | 28 | 54 | 67 | 25 | 60 | 49 |

in region II; this is also shown by the decrease in the fraction of infrared sources with an association.

We conclude that the objects in this region are mainly variable stars with oxygen-rich circumstellar shells that are more evolved than the objects in region II.

*Region IIIb:* The objects show a strong increase of the [25]–[60] colour as a function of the [12]–[25] colour. It suggests a further increase of the mass loss rate. About 90% of all LRS spectra show circumstellar emission from oxygen-rich dust shells. About 10% of the spectra are classified as spectra that show the 11.3 μm emission from carbon-rich dust shells according to the LRS classification. After visual inspection we conclude that the classification is doubtful: most of the spectra show weak 10 μm absorption and this mimics 11.3 μm emission. Therefore the sources belong in LRS class 31 or 32.

The variability average in this region is larger than in all others ($\langle VAR \rangle = 65$). The number of infrared sources that is associated with a variable star, however, is small (Table 2), which is not surprising because most of the objects are embedded in very thick dust/gas shells. A low fraction of infrared sources has an association with a stellar object.

We conclude that objects in this region are mainly variable stars with thick oxygen-rich circumstellar shells.

*Region IV:* This region contains objects with still larger [12]–[25] and [25]–[60] colours than in region IIIb, indicating stars with very large mass loss rates. The same is found from the LRS spectra: about 50% have very strong 10 μm absorption (only LRS classes 39 are found!). About 30% have redder spectra with sometimes weaker 10 μm absorption. Such spectra are expected when mass loss has recently stopped.

The variability average of these objects is lower than for the objects in regions IIIa/b and almost the same as for the objects in region II. The number of associations with a variable star is somewhat larger than in region IIIb. From Table 2 we also see that the fraction of infrared sources associated with a planetary nebula or an early type star with emission lines is significantly larger than in regions I to IIIb. The fraction of sources with an association is increased with respect to region IIIb which supports the idea that the central star already starts to shine through the circumstellar shell: mass loss probably has stopped and the shell is expanding and becomes transparent (Habing et al., 1987). We conclude that the objects in this region are mainly variable stars at the end of their mass loss phase that have very thick oxygen-rich circumstellar shells; a small fraction is already transformed into a planetary nebula.

*Region V:* The objects in this region have IR-colours that indicate very cold dust. Bedijn (1986) proved that their colours can not be obtained by a simple extrapolation from regions II–IV through increasing the mass loss rate; we discussed this point in Sect. 3.1. The IRAS colours correspond with a large detached circumstellar shell to which no new material is added at the inner radius: mass loss has stopped recently. About 70% of the LRS spectra found in this region show emission lines typical for planetary nebulae; they consist of hot ionized material close to the star and cool dust at large distances. About 30% do not show signs of ionisation but a weak to moderate 10 μm absorption. From Table 2 we see that 35% of the infrared sources are associated with a planetary nebula and 8% with an early type star with emission lines.

The variability average is low ($\langle VAR \rangle = 16$). Only 4% of the infrared sources are associated with a variable – or suspected variable star.

We conclude that these objects are mainly non-variable stars, probably stellar cores, with different temperatures ranging from a few thousand to more than 30,000 K which is necessary to ionize the surrounding material.

*Region VIa:* These objects have a large excess at 60 μm, but almost no excess at 25 or 12 μm. In more than 60% of the cases the LRS spectra have no infrared excess and in about 20% the weak 11.3 μm emission is seen, which indicates hot carbon-rich dust. About 10% of the spectra were classified as spectra with weak 10 μm absorption, but visual inspection failed to reveal the 10 μm absorption in any of them. From Table 2 we see that 24% of the objects are associated with a variable or a suspected variable star. In comparison with other regions, a large fraction of the sources is associated with a cool carbon star (19%). The variability average is low ($\langle VAR \rangle = 20$).

We conclude that the objects in this region are mainly non-variable stars with very cold dust at large distances. Some of them are carbon-rich; this is supported by the association of about 20% of the objects with a cool carbon star.

*Region VIb:* The objects have the same [12]–[25] colour as the objects in region IIIa, but a much larger [25]–[60] colour. It indicates that separate hot and cold dust components occur – a conclusion that argues against continuous mass loss, and favours the conclusion that the mass loss process has been interrupted for

some time. LRS spectra were only found for 5% of the objects and half of these show the 10 μm silicate band. For the others no distinction between carbon- or oxygen-rich dust can be found. From Table 2, however, we see that only 1% of the infrared sources is associated with a cool carbon star. Note that a relative large number of early type stars with emission lines is present (6%).

The variability average equals 36, the same value as for the objects in region II. The fraction of infrared sources associated with a variable star, however, is much smaller than in region II (8% versus 57%) which is probably caused by the fact that these objects are more obscured by circumstellar dust than the objects in region II – in agreement with the redder colours.

We conclude that these objects are variable stars of which a few have hot oxygen-rich material separated from far-away cold dust.

*Region VII:* The objects have the same [12]–[25] colours as in regions II and IIIa, but a [25]–[60] colour that is about 0.5 magnitude larger. This is typical for stars with carbon-rich dust shells, because carbon-rich dust shows a larger emissivity at wavelengths between 40 and 80 μm (e.g. Zuckerman and Dyck, 1986). Also LRS spectra show this: 30% have the 11.3 μm emission typical for carbon-rich dust. In 20% of the spectra the 10 μm emission feature is present indicating an oxygen-rich circumstellar shell and in the remaining 50% no distinction between carbon- and oxygen-rich dust can be made. From Table 2 we see that 11% of the infrared sources is associated with a cool carbon star and 2% with an S-star. The variability average is large ($\langle VAR \rangle = 41$). This agrees with the fact that 32% of the sources is associated with a variable or suspected variable star.

The objects found in this region are mainly stars with carbon-rich shells. There is still a significant fraction of oxygen-rich stars in this region.

*Region VIII:* According to the IR-colours this region contains very cool objects. They can be extreme cases of the objects found in the regions IV and V. About 60% of the LRS spectra show weak to moderate 10 μm absorption. The [25]–[60] colour, however, is in general too large for stars with circumstellar shells. About 30% of the LRS spectra are typical for planetary nebulae. From Table 2 we see that 3% of the infrared sources are associated with a planetary nebula and 4% with an early type star with emission lines. A relative large fraction (15%) is associated with galaxies. The variability of the infrared sources is moderate ($\langle VAR \rangle = 27$). We conclude that this region contains different types of objects.

## 4. An evolutionary scenario for AGB stars derived from the two-colour diagram

Based on the discussions so far we now give a possible scenario for stellar evolution at the AGB. After the termination of the hydrogen core burning on the main sequence a star moves via the First Giant Branch to the Horizontal Branch. Stars with masses smaller than about 10 $M_\odot$ develop a degenerate carbon-oxygen core and will first go through a phase of helium burning in a thin shell at the AGB (the so called E-AGB) until all helium is converted into carbon and oxygen and the star consists of a degenerate CO-core surrounded by a hydrogen envelope. Stars on the First Giant Branch and the E-AGB are non-variable and have spectral types ranging from K giants to M giants with temperatures between 2000 and 4000 K. In general they do not show an infrared excess and we conclude that the mass loss rate is still low. Because there is no infrared excess the objects can not be separated by their IRAS colours: for wavelengths larger than 10 μm the spectra are the Rayleigh-Jeans tail of the Planck curve and the colours are insensitive to temperature. We find these stars in region I of Fig. 5b. At a certain moment in the AGB life the mass loss rate increases drastically. The gap between regions I and II in Figs. 3a and 5a suggests a rapid increase in mass loss rate of a few orders of magnitude. This sudden increase in mass loss probably occurs during the TP-AGB phase, when the star is burning hydrogen and helium in a thin shell. The mechanism behind the increasing mass loss is sometimes thought to be dynamical pulsations and this is (to some extent) supported by the observations: the variability average of the objects in region II is significantly larger than in region I and the number of infrared sources associated with a variable star is about 60% in region II and only 11% in region I. In Sect. 3.2 we have shown that from the LRS spectra there is evidence for an "evolutionary track" from the Rayleigh-Jeans point (region I) via region II to region IIIa. The increase in infrared excess corresponds nicely with an increasing variability average (Fig. 4) – probably an indication of an increasing strength of the pulsations. In region IIIa we find stars with a 10 μm band – an indication of an oxygen-rich circumstellar shell. Mass loss rates for these stars are one of order $10^{-7} M_\odot$/yr. The variability average is very large (Table 1); there is a correlation with the strength of the 10 μm feature: a gradual increase in $\langle VAR \rangle$ from LRS-class 21 to 29 (see Fig. 4), but not with the IRAS colours: the LRS-classes 24 – 29 are concentrated around [12]–[25] = −0.5 and [25]–[60] = −1.9. Following the "evolutionary track" derived from observations of Miras and OH/IR stars we enter region IIIb, where we find a concentration of stars with 10 μm absorption: stars with thick oxygen-rich circumstellar shells and mass loss rates of a few times $10^{-5} M_\odot$/yr. The averaged variability of these stars is almost the same as for the stars in region IIIa. In Fig. 4 we see no correlation between variability and the strength of the 10 μm absorption. So either the strength of the pulsations has reached its maximum or the period has become so long that pulsations have escaped detection. At the end of the "evolutionary track" from Miras to OH/IR stars we enter region IV. Here the variability drops drastically suggesting a termination of the pulsation for at least about half of the objects. So here we find objects that have lost almost their entire hydrogen envelope and that transform into planetary nebulae. About 7% of the infrared sources are associated with a planetary nebula. According to Bedijn (1987) these objects should move to the right and enter region V, where the variability is still lower. In this region we find the largest fraction of infrared sources associated with a planetary nebula.

The scenario described above is likely to be the evolutionary scenario for a star with an oxygen-rich circumstellar shell at the top of the AGB. What happened to stars with carbon-rich circumstellar shells? There are two major possibilities: either these stars were already carbon-rich before the start of the dynamical pulsations (but this disagrees with the very low fraction of cool carbon stars and S-stars around the Raleigh-Jeans point (region I)), or the C/O ratio changed from a value smaller than unity to one larger. Such a change can occur when carbon-rich material is dredged up during a thermal pulse from regions very close to the hydrogen and helium burning zones. Evidence that this happened has been presented by Willems (1987), who suggests the following. If the star undergoes a thermal pulse the conditions for the dynamical pulsation will be disturbed during some time. If this interrupts the mass loss rate of the star for some time, then, as Willems showed, these stars describe an open loop in the IRAS two-colour diagram. First there is a displacement of the maximum in the energy distribution to longer wavelengths, but later the central star starts to dominate the spectrum again and the object

moves to the left in the diagram. The radius of the loop increases with increasing amount of mass in the circumstellar shell. The loops calculated by Willems start in region II or IIIa and go via region IIIb and VIb to region VIa; there a large fraction of infrared sources are associated with a cool carbon star. The model calculations by Willems show that the first part of the loop is passed in a very short time. A significant part of the sources in region VIa are carbon stars with cold, and probably oxygen-rich, dust at large distances. Then the dynamical pulsations start again and the stars show up in region VII where they show the 11.3 μm carbon emission. From Sect. 3.2 there is evidence that they move to the right, decrease the strength of the 11.3 μm emission and increase their variability: when the mass loss increases the shell becomes optically thick and the 11.3 μm emission disappears. As far as we know the 11.3 μm has never been detected in absorption but if such objects exist we expect them in the regions IIIa and IIIb at larger values of the [25]–[60] colour than the stars with oxygen rich envelopes. We expect that they will also move upwards to region IV and, after the termination of the pulsations, to region V to become a carbon-rich planetary nebula.

The foregoing scenario describes how a carbon star is born after a thermal pulse; and once the C/O ratio has been reversed it will remain reversed. However, it is unlikely that each thermal pulse produces a carbon star – after all a star may experience many thermal pulses. We suggest that an oxygen-rich star may survive thermal pulses for some time and that some oxygen-rich stars even survive all thermal pulses. Whether the C/O ratio in the envelope reverses will depend on several factors; the mass of the envelope – i.e. the region between the stellar core and the stellar photosphere – being one of them. If the envelope mass is large the mass in the circumstellar shell is relatively small; the star may recover from a thermal pulse as an oxygen-rich star and the loop in the two-colour diagram is small. Most of the time on the AGB the stars will be between thermal pulses and thus it will be at the "base" of the loop; we thus suggest that the "evolutionary track" from Miras to OH/IR stars is the lower envelope of the "looping" area. A part of the objects in region VIb are then candidates for stars that just have suffered a thermal pulse. Resuming we suggest that a star normally undergoes many relatively small loops, because the mass loss is interrupted for only a short time. Only when the C/O ratio reverses the mass loss is interrupted for a much longer time – probably because the chemistry in the envelope changes drastically – and the stars moves via region VIb to region VIa.

## 5. Conclusions

Using IRAS two-colour diagrams for the 12, 25, and 60 μm fluxes we have found evidence for an evolutionary sequence for stars with oxygen-rich circumstellar shells. Such evidence was found before for Mira variables and OH/IR stars (Bedijn, 1987). At the start of the dynamical pulsations the mass loss rate increases drastically. In about 100 years they form a circumstellar shell of hot matter, resulting in a change in [12]–[25] colour from −1.5 to −1.1; the [25]–[60] colour remains approximately the same. Following a sequence derived from IRAS observations of Mira variables and OH/IR stars, we see an increase of the [25]–[60] colour as a function of the [12]–[25] colour and this sequence represents an increase in mass loss rate. Because of the good correlation between the [25]–[60] and the [12–[25] colour, this increase can be described by one of the IRAS colours only, and the [12]–[25] colour seems to be the best choice. Along this sequence of oxygen rich stars we see an increase of the variability until variability reaches a maximum for the reddest sources. The stars with optical counter parts – e.g. Miras variables – show a rise in the variability if they become redder; the totally obscured stars – e.g. OH/IR stars – do not increase their variability with increasing [12]–[25] colour. The disappearance of the central source occurs around [12]–[25] = 0.2, the same point where the [25]–[60] colour starts to rise significantly. The termination of the mass loss phase seems to occur at a [12]–[25] colour between 1.2 and 1.5. For [12]–[25] colours larger than 1.5 we do not see oxygen-rich stars with large variability. Some of these objects were known as "non-variable" OH/IR stars, which may be the direct precursors of planetary nebulae (Habing et al., 1987; Van der Veen et al., 1987).

In the two-colour diagram we find stars above the "evolutionary track" from oxygen-rich Miras to OH/IR stars with a 60 μm flux that is too large to be caused by regular mass loss. We suggest that these stars have recently suffered a thermal pulse that suppressed for some time the dynamical pulsations and the mass loss. The stars describe a loop in the two-colour diagram, the radius of which depends on the mass of the circumstellar shell (Willems, 1987). During a thermal pulse the C/O ratio can be (but is not always) reversed because of the dredge up of carbon-rich material from the nuclear-burning zones: then the star becomes carbon-rich. After the restart of the dynamical pulsation it follows a track that is displaced to larger [25]–[60] colours with respect to the oxygen-rich stars caused by the difference in dust emissivity between 40 and 80 μm (Zuckerman and Dyck, 1986). Which fraction of oxygen-rich stars will become carbon-stars and how the transformation to a planetary nebula happens in detail is still not known, but deserves great attention because it is one of the most important problems of the evolution at the top of the AGB.

*Acknowledgements.* We thank J. Ober for making the photographs. W. van der Veen is supported by a grant from the Netherlands Organisation for the Advancement of Pure Research (ZWO).

## References

Baud, B., Habing, H.J.: 1983, *Astron. Astrophys.* **127**, 73
Bedijn, P.J.: 1987, *Astron. Astrophys.* **186**, 136
Chester, T.: 1986, in *Light from Dark Matter*, ed. F.P. Israel, Reidel, Dordrecht, p. 3
Habing, H.J., Van der Veen, W., Geballe, T.: 1987, in *Late Stages of Stellar Evolution*, eds. S. Kwok, S.R. Pottasch, Reidel, Dordrecht, p. 91
Herman, J., Burger, J.H., Penninx, W.: 1986, *Astron. Astrophys.* **167**, 247
IRAS, Explanatory Supplement: 1985, US Government Publication Office
IRAS, Point Source Catalogue: 1985, US Government Publication Office
IRAS, LRS Catalogue: eds. F.M. Olnon, E. Raimond: 1986, *Astron. Astrophys. Suppl. Ser.* **65**, 607
Neugebauer, G., et al.: 1984, *Astrophys. J. Letters* **278**, L1
Olnon, F.M., Baud, B., Habing, H.J., de Jong, T., Harris, S., Pottasch, S.R.: 1984, *Astrophys. J. Letters* **278**, L41
Rowan-Robinson, M., Lock, T.D., Walker, D.W., Harris, S.: 1986, *Monthly Notices Roy. Astron. Soc.* **222**, 273
Van der Veen, W., Habing, H.J., Geballe, T.R.: 1987, in *Planetary and Proto Planetary Nebulae: from IRAS to ISO*, ed. A. Preite-Martinez, Reidel, Dordrecht, p. 69
Willems, F.: 1987, Thesis, University of Amsterdam
Zuckerman, B., Dyck, H.M.: 1986, *Astrophys. J.* **311**, 345